

*Drosophila* type XV/XVIII Collagen, Mp, is involved in Wingless distribution

Ryusuke Momota <sup>a,\*</sup>, Ichiro Naito <sup>a</sup>, Yoshifumi Ninomiya <sup>b</sup> and Aiji Ohtsuka <sup>a</sup>

<sup>a</sup> Department of Human Morphology, Okayama University Graduate School of Medicine, Dentistry and Pharmaceutical Sciences

<sup>b</sup> Department of Molecular Biology and Biochemistry, Okayama University Graduate School of Medicine, Dentistry and Pharmaceutical Sciences

**\*Corresponding author:** Ryusuke Momota [momo@cc.okayama-u.ac.jp](mailto:momo@cc.okayama-u.ac.jp)

Address: Department of Human Morphology, 2-5-1, Shikata-cho, Kita ward, Okayama city, Okayama, Japan 7008558

Telephone: +81-86-235-7091 FAX: +81-86-235-7095

Authors declare no conflict of interest.

## **Abstract**

Multiplexin (Mp) is the *Drosophila* orthologue of vertebrate collagens XV and XVIII. Like them, Mp is widely distributed in the basement membranes of the developing embryos, including those of neuroblasts in the central and peripheral nervous systems, visceral muscles of the gut, and contractile cardioblasts. Here we report the identification of mutant larvae bearing *piggyBac* transposon insertions that exhibit decrease Mp production associated with abdominal cuticular and wing margin defects, malformation of sensory organs and impaired sensitivity to physical stimuli. Additional findings include the abnormal ultrastructure of fatbody associated with abnormal collagen IV deposition, and reduced Wingless deposition. Collectively, these findings are consistent with the notion that Mp is required for the proper formation and/or maintenance of basement membrane, and that Mp may be involved in establishing the Wingless signaling gradients in the *Drosophila* embryo.

## **Keywords**

Extracellular matrix, basement membrane, collagen, proteoglycan, chondroitin sulfate, Wingless/Wnt

**Abbreviations**

Hedgehog (Hh), chondroitin sulfate (CS), heparan sulfate (HS), thrombospondin-related (TSP), endostatin (ES)

**Contributors:** RM designed experiments, performed cloning of Mp cDNA, fly works, statistics and wrote the manuscript. IN made antiserum against Mp and wrote the manuscript. YN wrote the manuscript. AO performed electron microscopic analysis and wrote the manuscript.

## 1. Introduction

Extracellular matrix (ECM) proteins are fundamental structural components of all multicellular organisms. Basement membrane proteins in particular, are evolutionarily conserved across Protostomes and Deuterostome lineages (Fessler et al., 1987; Blumberg et al., 1988). Collagens type XV and XVIII are basement membrane-associated molecules that are grouped together as “multiplexin collagens”, a structurally distinct group within the larger family of collagen proteins (Ackley et al., 2001; Hynes and Zhao, 2000; Momota et al., 2008; Meyer and Moussian, 2009). Multiplexin collagens are characterized by glycosaminoglycan (GAG) side chains and an interrupted triple helix flanked by an N-terminal thrombospondin domain and a C-terminal endostatin domain (Myers et al., 1996; Halfter et al., 1998; Li et al., 2000; Dong et al., 2003). Additionally, the C-terminal 20-kDa cleavage product of collagen XVIII is believed to have a discrete function as an inhibitor of angiogenesis (O’Reilly et al., 1997). Collagen XV is preferentially found in skeletal and cardiac muscles, whereas collagen XVIII is mostly associated with subepithelial and subendothelial basement membranes (Myers et al., 1996, 2007; Halfter et al., 1998; Amenta et al., 2005; Carvalhaes et al., 2006; Tomono et al., 2002).

Mutations in human collagen XVIII lead to vitreoretinal degeneration, macular

abnormalities and occipital encephalocele in Knobloch syndrome (Sertié et al., 2000). Ocular manifestations and encephalocele are also found in mice lacking collagen XVIII (Fukai et al., 2002; Ylikärppä et al., 2003a; Utriainen et al., 2004; Marneros and Olsen, 2005). By contrast, mice lacking collagen XV exhibit skeletal myopathy and heart disease (Eklund et al., 2001). Consistent with the notion of separate functions in basement membrane physiology, mice without both collagens XV and XVIII do not display additional abnormalities (Ylikärppä et al., 2003b).

Similar findings have been reported for the invertebrate orthologues of collagen XV/XVIII, the nematode CLE-1 and the *Drosophila* multiplexin (Mp) gene product. While deletion of CLE-1 or Mp has no effect on organism viability, cell migration and axon guidance are abnormal, suggesting a role in cell migration and innervations (Ackley et al., 2001; Meyer and Moussian, 2009). This report further characterized the *Drosophila* Mp protein by examining its localization in the nervous systems and in the heart, and by characterizing the phenotype of hypomorphic Mp flies.

## **2. RESULTS**

### **2.1. Identification and molecular characterization of Mp and new splice variants**

**It was shown that the two electronically annotated genes CG33171 and CG8647**

comprise a single gene unit, *mp*, the *Drosophila* orthologue of vertebrate multiplexin collagen XV and XVIII and that the gene generates three major isoforms (Meyer and Moussian, 2009). In our database analysis, we have found that an EST clone “EST44112” contains the entire sequence of CG8647 with extra sequence at 5’ terminus, which were located at 12 kb upstream of CG8647 in the *Drosophila* genome. Accordingly, RNA extracted from wild type third-instar larvae was RT-PCR amplified using the foremost upstream sequence of EST44112 (primer S2) and the sequence corresponding to the fourth exon of CG33171 (primer AS2). The amplification reaction yielded a 1000 bp product that contains both EST44112 and CG33171 sequences, suggesting that the foremost upstream sequence is the first exon for *mp* and that the gene spans from 65D6 to 65E2 on *Drosophila* genome (Fig. 1A). Moreover, additional splice variants were identified that contain truncated TSP domain alone (Ap4) or TSP coupled with endostatin, which were separated with various lengths of collagenous sequences (Ap2, Af11) or non-collagenous sequences (Ap1, Ap3) (Fig. 1B and C).

## 2.2. Mp is a Chondroitin Sulfate Proteoglycan (CSPG)

Human collagens XV and XVIII carry chondroitin sulfate (CS) and heparin sulfate (HS) GAG side chains, respectively. *Drosophila* Mp has 9 Ser-Gly (SG)

consensus sites for GAG side chain attachment. Antibodies were therefore raised against the recombinant GST fusion protein corresponding to the hinge region of Mp in order to assess whether or not GAG chains are also present in the invertebrate collagen protein. Anti-Mp antisera recognized multiple bands ranging from 140 to 80 kDa (Fig. 2A, lane 1), which are absent in membranes incubated with pre-immune sera (Fig. 2A lanes 3 and 4) or are undetectable in protein extracts from *mp*<sup>f07253</sup>/*mp*<sup>f07253</sup> mutant flies (Fig. 2A, lanes 2 and 4).

Homogenates from wild-type flies were incubated with heparitinase or chondroitinase ABC, and the digests were analyzed by immunoblotting with anti-Mp sera. While heparitinase had no effect on the mobility of the immunoreactive material (Fig. 2B, H'ase), chondroitinase ABC treatment increased the intensity of multiple bands ranging from 120 to 145 kDa (Fig. 2B, Ch'ase).

### **2.3. Tissue distribution of the Mp protein**

Immunohistochemistry localized the strong Mp protein accumulation in both anterior and posterior midgut rudiment (arrowheads in Fig. 3A), and the neuroblasts of the anterior region appeared as dots along the germ band in stage 8 wild type embryos (arrows in Fig. 3A). At stage 14, Mp appeared both in the central and peripheral

nervous systems (CNS and PNS) (Fig. 3B). In the CNS, pairs of Mp-expressing cells appear to line up along the midline and are anteriorly adjacent to the anterior commissures in the dorsal side of the neuropile (arrowheads in Fig. 3B). Another group of cells that express Mp was located on the midline between the anterior and posterior commissures and on the ventral side of the neuropile (Fig. 3B). Distribution of Mp did not correspond with either the pan-neuronal marker anti-HRP antigen (Fig. 3C) or Engrailed (Fig. 3D). At later stages of development, Mp was found to decorate the neuropile in a ladder like structure, implying that the axons of these cells are crossing the midline and are connecting longitudinally (Fig. 3E). By its morphology and its origin from Engrailed-negative midline cells, we believe that these Mp expressing cells are interneuron precursors (Bossing and Brand, 2006). The finding that axons stained with anti-Mp extend from the proneural clusters toward the CNS (arrows, Fig. 3G) supported the notion that Mp is expressed in the bipolar sensory neuron of the PNS. Mp expression is also noticeable in organs of mesenchymal origin, such as visceral muscle or dorsal vessel, fly heart (Fig. 3F, G). Interestingly, Mp expression is prominent in the cardioblasts and alary muscle in the heart region, but is absent in the ostia, the inflow tract of the *Drosophila* heart (Fig. 3G, H).



## 2.4. Identification and characterization of *mp* hypomorphic flies

Two *piggyBac* transposon elements that carry splice-trapping insertion alleles (referred to as *mp*<sup>f07253</sup> and *mp*<sup>f03008</sup>) were identified in the Harvard Exelixis collections (Fig. 1A). Likewise the previously reported two deletion *mp* mutant flies, these mutant flies are viable and fertile and lack overt phenotypes even in homozygosity (Meyer and Moussian, 2009). RNA was therefore extracted from third-instar larvae to assess the possible presence of one or more *mp* transcripts in each of the homozygous mutant lines by RT-PCR using several combinations of primers. The assay revealed a faint expression of *mp*-A and *mp*-B transcripts only with a pair of primers ES and AS4 in both mutant homozygotes, suggesting that the *Mp* alleles represent hypomorphic mutations with trace transcripts of endostatin region rather than null mutations (Fig. 1B and 4A). The apparent discrepancy between immunoblots and PCR analyses is likely to reflect the sensitivity of the two techniques (Figs. 2A and 4A).

Axon pathfinding errors have been previously reported in *Drosophila mp* deletion mutants (Meyer and Moussian, 2009) and in CLE-1 mutant nematodes (Ackley et. al., 2001). We therefore examined axonal migration in our *mp* mutants by staining embryos with a pan-neuronal marker and found seemingly normal neural morphology consistent with the hypomorphic nature of the *mp*<sup>f07253</sup> and *mp*<sup>f03008</sup> alleles

(data not shown). By contrast wing margin and abdominal segment cuticle defects were readily evident in these mutant flies (Fig. 4B). Specifically, the wing longitudinal veins were not fully extended to the edge (Fig. 4B, B') and the hemisegments of the dorsal abdominal cuticle plates (tergites) were either missing or were not fused at the dorsal midline (Fig. 4C'). Importantly, these phenotypes were no longer observed after excising the *piggyBac* transposons (data not shown). Although lacking direct evidence, Wingless specification of wing morphogenesis and tergite cell fates determination suggest the potential association of wing and cuticle defects in *mp* hypomorphic flies with impaired Wingless signaling (Phillips and Whittle, 1993; Shirras and Couso, 1996; Kopp et al, 1999).

## **2.5. Mp mutants exhibit blunt sensory neurons and less sensitivity to physical stimuli**

Observational evidence suggested that mutant larvae may not be able to sense physical stimuli enough to avoid colliding with one another. To test this hypothesis, we performed a touch sensitivity assay on mutant and control third-instar larvae. Wild type larvae exhibited strong avoidance to physical stimuli ( $\bar{x} = 12.87$ ), whereas mutants had poor response to them (*mp*<sup>f03008</sup>/*mp*<sup>f03008</sup>:  $\bar{x} = 8.93$ , *mp*<sup>f07253</sup>/*mp*<sup>f07253</sup>:  $\bar{x} = 4.65$ ) (Fig. 5A). We stained embryos with 22c10 and found that mutants exhibited blunt

morphology in the neurons of chordotonal organs (Fig. 5B, B'). This result was in line with Mp distribution in the proneural clusters of the fly embryo (Fig. 3G); together, these findings implicated the Mp protein **is required** for proper neuronal morphology and function.

## 2.6. Altered lipid accumulation in Mp mutants

Larval fatbodies were smaller and lipid droplets were larger in  $mp^{f07253}/mp^{f07253}$  and  $mp^{f03008}/mp^{f03008}$  flies compared to wild type flies (Fig. 5C, C'). Mp decorates the cell boundaries of the fatbody suggesting a probable defect in basement membrane structure (data not shown). To test this hypothesis, basement membranes were visualized by immunostaining for Viking, a *Drosophila*  $\alpha 2(\text{IV})$  collagen. The analysis revealed a significant disorganization of cell boundaries in  $mp^{f07253}/mp^{f07253}$  flies, suggesting a failure to assemble basement membranes (Fig. 5D, D'). A similar result was obtained using  $mp^{f07253}/mp^{f07253}$  flies producing GFP fused to Viking (data not shown). At the ultrastructural level, the intercellular spaces were broader in mutants than wild type flies (Fig. 5E, E'), possibly because lost integrity of basement membranes failed to provide proper scaffold to cells. Thus, Mp might be involved in the formation/maintenance of the fatbody basement membrane and by extension, in

regulating lipid metabolism.

## 2.7. Mp Deficiency mitigates Wingless deposition

Mp expression in cardioblasts and its absence in the ostia are complementary to Wingless expression (Fig. 3G, H). We therefore asked whether Mp may affect Wingless localization and found that the overall distribution of Wingless is diminished in mutant embryos (Fig. 6A, A'). Particularly remarkable was the decrease of Wingless in the larval proventriculus (Fig. 6B, B') where Mp is expressed in the adjacent circumferential muscle (Fig. 6C, C'). Wingless activity is required for cell migration to occur from the foregut into the endodermal pouch during proventriculus morphogenesis. In  $mp^{f07253}/mp^{f07253}$  flies this process was not hampered by the severe reduction in Wingless, suggesting that residual Wingless deposition might be enough to complete proventriculus organogenesis.

## 3. Discussion

Multiple isoforms of collagen XVIII are present in vertebrates as a result of alternative tissue-specific promoters and splicing mechanisms (Rehn and Pihlajaniemi, 1995). Recently, three isoforms of the *Drosophila* equivalent of vertebrate collagen

XV/XVIII have been reported (Meyer and Moussian, 2009). In this paper, we have identified another series of splice variants. The expression and the function of the new isoforms remain to be elucidated as some of them do not contain the epitope region of our anti-Mp antibody. It is however conceivable to argue that they may account for the residual transcription of the ES domain found in the deletion mutant  $mp^{\Delta N4-11}$ , as the deleted region is spliced out in these transcripts (Meyer and Moussian, 2009).

Our immunoblots analysis revealed Mp protein increased the intensity of the longer (120-145 kDa) isoforms after chondroitinase ABC treatment. We interpreted these results to indicate that the longer, but not the shorter, Mp isoforms are predominantly modified by GAG side chains and that the modifications largely correspond to CS rather than HS side chains. To our knowledge, this is the first biochemical validation of the postulated presence of CSPG in *Drosophila* (Cássaro and Dietrich, 1977; Pinto et al., 2004).

As observed in other species such as zebrafish and nematode, *mp* gene is preferentially expressed in the nervous system and in the muscular system (Ackley et al., 2001; Pagnon-Minot et al., 2008; Haftek et al., 2003; Meyer and Moussian, 2009). In this report, we observed Mp protein accumulations in the developing CNS and PNS in a segmental cellular fashion. Mp protein was observed at embryonic stage 8, which was

earlier than the previous expression data (Meyer and Moussian, 2009). The discrepancy is possibly derived from the sensitivity of the detection methods: the previous observation was done *in situ* hybridization probing for isoforms A specific region while the epitope region of our anti-Mp was common in both A and B isoforms. We presume that the cells, even though with a low transcriptional activity, were continuously secreting Mp, which was accumulated enough to be detected in our system.

Collagen XV deficient mice manifest endothelial cell degeneration in the heart and collagen XVIII is thought to be involved in cardiac valve formation (Eklund et al., 2001; Carvalhaes et al., 2006). Dorsal vessel formation in *Drosophila* shares many similarities with vertebrate heart development (Zaffran et al., 2006; Zaffran and Frasch, 2002; Tao and Schulz, 2007). The present study documented the restricted expression of Mp in the contractile cardioblasts of the heart, which also express the transcriptional determinant of heart development Tinman (Bour et al., 1995; Lilly et al., 1994, 1995; reviewed in Potthoff and Olson, 2007). Interestingly, the 5' upstream region of the *mp* gene contains multiple Tinman binding sites, as well as recognition sequences for the myogenic factor Mef-2 (data not shown). It is therefore tempting to argue that *mp* gene expression during myogenesis may be under the direct control of

Tinman and Mef-2.

It has been suggested that collagen XVIII may antagonize Wnt signaling owing to the presence of a polypeptide sequence with strong homology to the Wnt receptor, Frizzled (Quélard et al., 2008). Hypomorphic Mp mutants exhibit manifestations similar to those caused by *wingless* loss-of-function mutations; additionally, Wingless distribution is markedly reduced in these Mp mutant flies. **We assume that the existence of Mp itself affects the morphogen gradient and the low availability of Mp in the hypomorphic mutants results in mild phenotypes in wing margin and tergite formation.** These lines of correlative evidence strongly suggest that multiplexin collagens may be required for the proper Wnt signaling in both vertebrate and invertebrate organisms. Although the mechanism is yet to be clarified, one possible explanation is that the CS chains of Mp may establish Wingless signaling area by modulating ligand diffusion. Alternatively, the CS chains of Mp may mediate signaling between Hh and Wingless, as they are both lipid-modified proteins that share similarities in signaling mechanisms (Nusse, 2003). Indeed, the area of Hh signaling was expanded in zebrafish embryos in which collagen XV expression was silenced (Pagnon-Minot et al., 2008). Furthermore, it has been shown that Hh ligands are concentrated on CS and attracted to HS by its higher affinity on target cells (Cortes et

al., 2009).

Altered lipid storage in the mutant fatbody is reminiscent of lipid accumulation in the aorta of *Col18a1* (-/-) mice and altered serum lipid contents in Knobloch syndrome patients (Moulton et al., 2004; Esko et al., 2008). In addition, Errera et al. (2008) have recently reported upregulation of *COL18A1* gene expression during in vitro adipogenesis and genetic linkage between Frizzled polymorphisms and obesity. Furthermore, Hh and Wnt signaling have been demonstrated to be important regulators in adipocyte differentiation (Ross et al., 2000; Fontaine et al., 2008). It is therefore possible that Mp may influence adipocyte differentiation through these signaling pathways.

## 4. Experimental Procedures

### 4.1 *Drosophila* stocks

Oregon-R, P{wg-lac-z} / CyO and Vkg-GFP flies (G00454; Morin et al., 2001) were obtained from *Drosophila* Genetic Resource Center (DGRC, Kyoto Institute of Technology). PBac{WH}f07253 and PBac{WH}f03008 (Thibault et al., 2004) were obtained from Harvard Exelixis collection (Boston, MA). Revertants from the *piggyBac* insertion were generated by excision of the transposon and were selected for the white-



eye individuals. Oregon-R was used as wild type control otherwise indicated. Flies were raised at room temperature.

#### 4.2. cDNA cloning and characterization of *mp* gene

A cDNA clone (GH14382), containing an electronically annotated gene CG33171-RE, was obtained from *Drosophila* Genomics Resource Center (DGRC, Bloomington, IN). For cloning *mp*-A cDNA upstream region, one microgram of total RNA extracted from third instar larvae was reverse transcribed with ReverTra Ace and random hexamer (Toyobo, Japan), and 1/100 of resultant cDNA was used as a template for PCR using S2 (5'-CTTTGTGGCTCCTGCTTTGT-3') or S0 (5'-CTGTTCAAGATGCGTGTGCT-3') with AS2 (5'-CTCCCTTCTCGCCCTTGAT-3'). The PCR products (S0/AS2) were cloned into pCRII vector (Invitrogen, Carlsbad, CA), designated as RM8B. Two primer sets, S0 with AS1 (5'-GGCAATCGAGTTCCAATTGT-3') and BS1 (5'-CGATTGCCGTTGTAAAAGT-3') with BAS1 (5'-CCGAGCAGGAAGAACAGAAT-3'), were used to amplify each isoform characteristic region. The obtained cDNA fragments were cloned into pCRII vector as described above, designated as *mp*-A/TA and *mp*-B/TA, respectively. To amplify the endostatin encoding region, we used ES (5'-CTACGCGTGGCCGCACTGAAT-3') with AS4 (5'-

AGCAGTAAATTTTCTAAATGCGC-3'). The primers S2, S0 and AS1 were designed based on sequence of the EST clone 44112 (accession number: EC199544) which contained sequence of CG8647. The primers BS1, BAS1, AS2, ES and AS4 were designed based on sequence of CG33171. The locations of these specific primers were shown in Figure 1B. **The sequences of various isoforms were submitted to GenBank.** The primers *rp49s* (5'-ATGACCATCCGCCAGCATAC-3') and *rp49as* (5'-CTGCATGAGCAGGACCTCCAG-3') amplified *rp49*, a constitutive gene in *Drosophila*, were used as a reference for the RT-PCR quantification analysis. The gel image was processed for densitometry analysis using ImageJ gel analysis function (NIH, Bethesda, MD) and ***mp* gene expression level was normalized to the level of *rp49* and was compared between the lines.**

#### **4.3. Production of antiserum**

The *mp* NC1 domain nucleotide sequences were amplified from cDNA clone GH14382 (DGRC, Bloomington, IN) using 5rep and 3rep. The PCR products were introduced into pGEX-6P-1 vector (GE healthcare, Little Chalfont, UK) using BamHI and EcoRI sites and confirmed by sequencing. This GST-fusion expression construct was introduced into *Escherichia coli* strain BL21 and protein purification was

performed using Glutathione Sepharose 4B (GE healthcare, Little Chalfont, UK) according to manufacturer's instruction. Purified protein was injected into Balb/c mice. The resulting antibodies were affinity purified from sera by binding to CNBr-activated Sepharose (GE healthcare, Little Chalfont, UK) coated with Mp collected from cleavage of fusion protein with PreScission protease (GE healthcare, Little Chalfont, UK) and were used for staining and immunoblotting. All procedures relating animals were approved by Okayama University's Animal Care and Use Committee and carried out in accordance with the Guidelines for Animal Experiments at Okayama University. Care was taken to minimize their suffering.

#### **4.4. Protein extraction and digestion with glycosidase**

Fifty adult flies were homogenized in 2 ml of Urea buffer (50 mM Tris-HCl (pH 8.0), 10 mM EDTA, 150 mM NaCl, 6 M Urea, 0.1% Triton X-100), extracted with rotation for overnight at 4 °C and centrifuged at 12,000 rpm for 10 min to collect supernatant (1200 µl). After dialysis against appropriate buffer for each enzyme, the adult extracts (50 µl) were incubated with Chondroitinase ABC (20 mU) or heparitinase (2 mU) (Seikagaku Kogyo, Tokyo, Japan) for 3 h at 37 °C. The reaction was stopped by adding SDS sample buffer with 2-mercaptoethanol, samples were

denatured for 5 min at 100 °C and resolved on 6% SDS-PAGE.

#### **4.5. Antibodies**

Antiserum against Mp (1:250 for immunohistochemistry; 1:500 for Western blots) was used for the detection of Mp. Anti-22c10 (1:10), Anti-Wingless (4D4, 1:50) and anti-Engrailed/inv (4D9, 1:3) were obtained from Developmental Studies Hybridoma Bank (DSHB, Iowa City, IA). As secondary antibodies, anti-mouse IgG-alkaline-phosphatase (1:500; Promega, Madison, WI) or LSAB2 (DAKO, Glostrup Denmark) was used and detection was done according to the manual. Larval organs were obtained from dissected third instar larvae and fixed with 4% paraformaldehyde (PFA) in phosphate buffered saline (PBS: 2 mM NaH<sub>2</sub>PO<sub>4</sub>, 8 mM Na<sub>2</sub>HPO<sub>4</sub>, 170 mM NaCl, pH 7.4) for 20 min. Blocking was done for 1 h in 4% skim milk in PBS and incubation of primary antibodies was done overnight at 4 °C.

#### **4.6. Microscopy and image processing**

Fluorescent and phase contrast images were obtained using a microscopy (Olympus, Tokyo, Japan) equipped with Zeiss Axiovision. Confocal images were obtained using Zeiss LSM510. Larval locomotion were recorded using a dissection

microscopy (Olympus, Tokyo, Japan) equipped with CCD camera and were processed using Premier 6.0 (Adobe, San Jose, CA).

#### **4.7. Touch sensitivity assays**

Classifications of reactions were performed as previously described (Caldwell et al., 2003). Student's *t*-test ( $P < 0.05$ ) was performed using JMP7 (SAS Institute Inc., Cary, NC) for statistical analysis.

#### **4.8. Transmission Electron Microscopy**

Larval fatbodies were immersion-fixed with 2.5% glutaraldehyde/4% PFA in 0.1 M phosphate buffer (pH 7.3). After dehydration with ethanol series, the samples were embedded in epoxy resin, cut into ultrathin sections and observed with a transmission electron microscope (H-7100, Hitachi, Tokyo, Japan).

#### **Acknowledgements**

We thank our colleagues in the laboratory of HM and MBB for a variety of contributions and for critical discussions, Masahiro Narasaki for his excellent skills in electron microscopy, the central core facility in Okayama Univ. Med. School for

technical assistance. We are grateful to Dr. Francesco Ramirez for helpful advice and proofreading and Drs. John and Lisa Fessler for helpful advice, providing antibodies and stimulating discussions. The fly stocks were obtained from *Drosophila* Genetic Resource Center at Kyoto Institute of Technology, Bloomington stock center and the Exelixis Collection at the Harvard Medical School.

## References

Ackley, B. D., Crew, J. R., Elamaa, H., Pihlajaniemi, T., Kuo, C. J., Kramer, J. M., 2001. The NC1/endostatin domain of *Caenorhabditis elegans* type XVIII collagen affects cell migration and axon guidance. *J. Cell Biol.* 152, 1219-1232.

Ackley, B. D., Kang, S. H., Crew, J. R., Suh, C., Jin, Y., Kramer, J. M., 2003. The basement membrane components nidogen and type XVIII collagen regulate organization of neuromuscular junctions in *Caenorhabditis elegans*. *J. Neurosci.* 23, 3577-3587.

Amenta, P. S., Scivoletti, N. A., Newman, M. D., Sciancalepore, J. P., Li, D., Myers, J. C., 2005. Proteoglycan-collagen XV in human tissues is seen linking banded collagen fibers subjacent to the basement membrane. *J. Histochem. Cytochem.* 53, 165-176.

Blumberg, B., MacKrell, A. J., Fessler, J. H., 1988. *Drosophila* basement membrane procollagen  $\alpha 1$  (IV). II. Complete cDNA sequence, genomic structure, and general implications for supramolecular assemblies. *J. Biol. Chem.* 263, 18328-18337.

Bossing, T., Brand, A. H., 2006. Determination of cell fate along the anteroposterior axis of the *Drosophila* ventral midline. *Development* 133, 1001-1012.

Bour, B. A., O'Brien, M. A., Lockwood, W. L., Goldstein, E. S., Bodmer, R., Taghert, P. H., Abmayr, S. M., Nguyen, H. T., 1995. *Drosophila* MEF2, a transcription factor that is

essential for myogenesis. *Genes Dev.* 9, 730-741.

Caldwell, J. C., Miller, M. M., Wing, S., Soll, D. R., Eberl, D. F., 2003. Dynamic analysis of larval locomotion in *Drosophila* chordotonal organ mutants. *Proc Natl Acad Sci U. S. A.* 100, 16053-16058.

Carvalhaes, L. S., Gervásio, O. L., Guatimosim, C., Heljasvaara, R., Sormunen, R., Pihlajaniemi, T., Kitten, G. T., 2006. Collagen XVIII/endostatin is associated with the epithelial-mesenchymal transformation in the atrioventricular valves during cardiac development. *Dev. Dyn.* 235, 132-142.

Cortes, M., Baria, A. T., Schwartz, N. B., 2009. Sulfation of chondroitin sulfate proteoglycans is necessary for proper Indian hedgehog signaling in the developing growth plate. *Development* 136, 1697-1706.

Cássaro, C. M., Dietrich, C. P., 1977. Distribution of sulfated mucopolysaccharides in invertebrates. *J. Biol. Chem.* 252, 2254-2261.

Dong, S., Cole, G. J., Halfter, W., 2003. Expression of collagen XVIII and localization of its glycosaminoglycan attachment sites. *J. Biol. Chem.* 278, 1700-1707.

Eklund, L., Piuhola, J., Komulainen, J., Sormunen, R., Ongvarrasopone, C., Fässler, R., Muona, A., Ilves, M., Ruskoaho, H., Takala, T. E., Pihlajaniemi, T., 2001. Lack of type XV collagen causes a skeletal myopathy and cardiovascular defects in mice. *Proc. Natl.*



Acad. Sci. U. S. A. 98, 1194-1199.

Errera, F. I. V., Canani, L. H., Yeh, E., Kague, E., Armelin-Corrêa, L. M., Suzuki, O. T., Tschiedel, B., Silva, M. E. R., Sertié, A. L., Passos-Bueno, M. R., 2008. COL18A1 is highly expressed during human adipocyte differentiation and the SNP c.1136C > T in its "frizzled" motif is associated with obesity in diabetes type 2 patients. An. Acad. Bras. Cienc. 80, 167-177.

Esko, J. D. Bishop, J. R., Passos-Bueno, M. R., Stanford, K. I., Yeh, E., Witztum, J. L., Bensadoun, A., Moulton, K. S., 2008. Hypertriglyceridemia caused by mutation of the basement membrane proteoglycan Type XVIII collagen. Matrix Biol. 27(Supplement 1), 12-12.

Fessler, L., Campbell, A., Duncan, K., Fessler, J., 1987. Drosophila laminin: characterization and localization. J. Cell Biol. 105, 2383-2391.

Fontaine, C., Cousin, W., Plaisant, M., Dani, C., Peraldi, P., 2008. Hedgehog signaling alters adipocyte maturation of human mesenchymal stem cells. Stem Cells 26, 1037-1046.

Fukai, N., Eklund, L., Marneros, A. G., Oh, S. P., Keene, D. R., Tamarkin, L., Niemelä, M., Ilves, M., Li, E., Pihlajaniemi, T., Olsen, B. R., 2002. Lack of collagen XVIII/endostatin results in eye abnormalities. EMBO J. 21, 1535-1544.

Haftak, Z., Morvan-Dubois, G., Thisse, B., Thisse, C., Garrone, R., Le Guellec, D., 2003. Sequence and embryonic expression of collagen XVIII NC1 domain (endostatin) in the zebrafish. *Gene Expr. Patterns* 3, 351-354.

Halfter, W., Dong, S., Schurer, B., Cole, G. J., 1998. Collagen XVIII is a basement membrane heparan sulfate proteoglycan. *J. Biol. Chem.* 273, 25404-25412.

Hynes, R. O., Zhao, Q., 2000. The evolution of cell adhesion. *J. Cell Biol.* 150, F89-F96.

Kopp, A., Blackman, R. K., Duncan, I., 1999. Wingless, Decapentaplegic and EGF Receptor signaling pathways interact to specify dorso-ventral pattern in the adult abdomen of *Drosophila*. *Development* 126, 3495-3507.

Li, D., Clark, C. C., Myers, J. C., 2000. Basement membrane zone type XV collagen is a disulfide-bonded chondroitin sulfate proteoglycan in human tissues and cultured cells. *J. Biol. Chem.* 275, 22339-22347.

Lilly, B., Galewsky, S., Firulli, A. B., Schulz, R. A., Olson, E. N., 1994. D-MEF2: a MADS box transcription factor expressed in differentiating mesoderm and muscle cell lineages during *Drosophila* embryogenesis. *Proc. Natl. Acad. Sci. U. S. A.* 91, 5662-5666.

Lilly, B., Zhao, B., Ranganayakulu, G., Paterson, B., Schulz, R., Olson, E., 1995. Requirement of MADS domain transcription factor D-MEF2 for muscle formation in *Drosophila*. *Science* 267, 688-693.

Marneros, A. G., Keene, D. R., Hansen, U., Fukai, N., Moulton, K., Goletz, P. L., Moiseyev, G., Pawlyk, B. S., Halfter, W., Dong, S., Shibata, M., Li, T., Crouch, R. K., Bruckner, P., Olsen, B. R., 2004. Collagen XVIII/endostatin is essential for vision and retinal pigment epithelial function. *EMBO J.* 23, 89-99.

Marneros, A. G. and Olsen, B. R., 2005. Physiological role of collagen XVIII and endostatin. *FASEB J.* 19, 716-728.

Meyer, F and Moussian, B., 2009. *Drosophila* multiplexin, (Dmp) modulates motor axon pathfinding accuracy. *Dev. Growth Differ.* 51, 483-498.

Momota, R., Naito, I., Ninomiya, Y., Ohtsuka, A., 2008. Characterization of drole, *Drosophila* type XV/XVIII collagen. *Matrix Biol.* 27(Supplement 1), 23-24.

Morin, X., Daneman, R., Zavortink, M., Chia, W., 2001. A protein trap strategy to detect GFP-tagged proteins expressed from their endogenous loci in *Drosophila*. *Proc. Natl. Acad. Sci. U. S. A.* 98, 15050-15055.

Moulton, K. S., Olsen, B. R., Sonn, S., Fukai, N., Zurakowski, D., Zeng, X., 2004. Loss of collagen XVIII enhances neovascularization and vascular permeability in atherosclerosis. *Circulation* 110, 1330-1336.

Myers, J. C., Amenta, P. S., Dion, A. S., Sciancalepore, J. P., Nagaswami, C., Weisel, J. W., Yurchenco, P. D., 2007. The molecular structure of human tissue type XV presents a

unique conformation among the collagens. *Biochem. J.* 404, 535-544.

Myers, J. C., Dion, A. S., Abraham, V., Amenta, P. S., 1996. Type XV collagen exhibits a widespread distribution in human tissues but a distinct localization in basement membrane zones. *Cell Tissue Res.* 286, 493-505.

Nusse, R., 2003. Wnts and Hedgehogs: lipid-modified proteins and similarities in signaling mechanisms at the cell surface. *Development* 130, 5297-5305.

O'Reilly, M. S., Boehm, T., Shing, Y., Fukai, N., Vasios, G., Lane, W. S., Flynn, E., Birkhead, J. R., Olsen, B. R., Folkman, J., 1997. Endostatin: an endogenous inhibitor of angiogenesis and tumor growth. *Cell* 88, 277-285.

Pagnon-Minot, A., Malbouyres, M., Haftek-Terreau, Z., Kim, H. R., Sasaki, T., Thisse, C., Thisse, B., Ingham, P. W., Ruggiero, F., Guellec, D. L., 2008. Collagen XV, a novel factor in zebrafish notochord differentiation and muscle development. *Dev. Biol.* 316, 21-35.

Phillips, R. G. and Whittle, J. R. S., 1993. *wingless* expression mediates determination of Peripheral nervous system elements in late stages of *Drosophila* wing disc development. *Development* 118, 427-438.

Pinto, D. O., Ferreira, P. L., Andrade, L. R., Petrs-Silva, H., Linden, R., Abdelhay, E., Araujo, H. M. M., Alonso, C. V., Pavao, M. S., 2004. Biosynthesis and metabolism of

sulfated glycosaminoglycans during *Drosophila melanogaster* development.

Glycobiology 14, 529-536.

Potthoff, M. J., Olson, E. N., 2007. MEF2: a central regulator of diverse developmental programs. Development 134, 4131-4140.

Quélard, D., Lavergne, E., Hendaoui, I., Elamaa, H., Tirola, U., Heljasvaara, R., Pihlajaniemi, T., Clément, B., Musso, O., 2008. A cryptic frizzled module in cell surface collagen 18 inhibits Wnt/beta-catenin signaling. PLoS One 3, e1878.

Rehn, M. and Pihlajaniemi, T., 1995. Identification of Three N-terminal Ends of Type XVIII Collagen Chains and Tissue-specific Differences in the Expression of the Corresponding Transcripts. J. Biol. Chem. 270, 4705-4711.

Ross, S. E., Hemati, N., Longo, K. A., Bennett, C. N., Lucas, P. C., Erickson, R. L., MacDougald, O. A., 2000. Inhibition of adipogenesis by Wnt signaling. Science 289, 950-953.

Sertié, A. L., Sossi, V., Camargo, A. A., Zatz, M., Brahe, C., Passos-Bueno, M. R., 2000. Collagen XVIII, containing an endogenous inhibitor of angiogenesis and tumor growth, plays a critical role in the maintenance of retinal structure and in neural tube closure (Knobloch syndrome). Hum Mol Genet 9, 2051-2058.

Shirras, A. D., and Couso, J. P., 1996. Cell Fates in the Adult Abdomen of *Drosophila*

Are Determined by *wingless* during Pupal Development. *Dev. Biol.* 175, 24-36.

Tao, Y., Schulz, R. A., 2007. Heart development in *Drosophila*. *Seminars in Cell, Dev. Biol.* 18, 3-15.

Thibault, S. T., Singer, M. A., Miyazaki, W. Y., Milash, B., Dompe, N. A., Singh, C. M., Buchholz, R., Demsky, M., Fawcett, R., Francis-Lang, H. L., Ryner, L., Cheung, L. M., Chong, A., Erickson, C., Fisher, W. W., Greer, K., Hartouni, S. R., Howie, E., Jakkula, L., Joo, D., Killpack, K., Laufer, A., Mazzotta, J., Smith, R. D., Stevens, L. M., Stuber, C., Tan, L. R., Ventura, R., Woo, A., Zakrajsek, I., Zhao, L., Chen, F., Swimmer, C., Kopczynski, C., Duyk, G., Winberg, M. L., Margolis, J., 2004. A complementary transposon tool kit for *Drosophila melanogaster* using P and *piggyBac*. *Nat. Genet.* 36, 283-287.

Tomono, Y., Naito, I., Ando, K., Yonezawa, T., Sado, Y., Hirakawa, S., Arata, J., Okigaki, T., Ninomiya, Y., 2002. Epitope-defined monoclonal antibodies against multiplexin collagens demonstrate that type XV and XVIII collagens are expressed in specialized basement membranes. *Cell Struct. Funct.* 27, 9-20.

Utriainen, A., Sormunen, R., Kettunen, M., Carvalhaes, L. S., Sajanti, E., Eklund, L., Kauppinen, R., Kitten, G. T., Pihlajaniemi, T., 2004. Structurally altered basement membranes and hydrocephalus in a type XVIII collagen deficient mouse line. *Hum. Mol.*

Genet. 13, 2089-2099.

Ylikärppä, R., Eklund, L., Sormunen, R., Kontiola, A. I., Utriainen, A., Määttä, M., Fukai, N., Olsen, B. R., Pihlajaniemi, T., 2003a. Lack of type XVIII collagen results in anterior ocular defects. *FASEB J.* 17, 2257-2259.

Ylikärppä, R., Eklund, L., Sormunen, R., Muona, A., Fukai, N., Olsen, B. R., Pihlajaniemi, T., 2003b. Double knockout mice reveal a lack of major functional compensation between collagens XV and XVIII. *Matrix Biol.* 22, 443-448.

Zaffran, S., Frasch, M., 2002. Early signals in cardiac development. *Circ. Res.* 91, 457-469.

Zaffran, S., Reim, I., Qian, L., Lo, P. C., Bodmer, R., Frasch, M., 2006. Cardioblast-intrinsic Tinman activity controls proper diversification and differentiation of myocardial cells in *Drosophila*. *Development* 133, 4073-4083.

## Figure legends

Figure 1. Gene and protein structure of Mp. (A) Computationally annotated genes CG8647 and CG33171, mapped on chromosome 3L from 65D6 to 65E2, comprise a single gene, *mp*. (B) The exon/intron organization of *mp* and transposon insertion sites. Splicing variants with TSP (*mp*-A, above) and without TSP (*mp*-B, below) were indicated along with the exon/intron diagram. Alternative splicings of Mp-A isoforms (p1-4, fl1) were indicated by labeled curved arrows. Splicing sites which occurs in the middle of exons were indicated by vertical bars. ATG: the first methionine, TGA-p4: specific termination codon for Ap4, TAA: termination codon. The regions amplified by RT-PCR (underlined), the skipped exons of each transcript (dashed line) and the locations of primers (horizontal arrows). The colors indicate the corresponding protein domain: untranslated region (black), TSP (red), junction (green), collagenous domain (blue) and endostatin (yellow). The sequence used for antigen production was indicated by upward bracket. (C) Protein structure: Mp-A isoforms (p3, p1, p4, p2, fl1) and Mp-B. Each color refers to the protein domain described above.

Figure 2. (A) Immunoblot of adult fly extracts from wild type (lane 1, 3) and  $mp^{f07253}/mp^{f07253}$  (lane 2, 4). Major immunoreactive bands (80 kD: arrow, 140 kD: arrowhead) appeared in wild type crude extract (lane 1) which is missing in  $mp^{f07253}/mp^{f07253}$  sample (lane 2). None of



these bands were detected by preimmune antiserum (lane 3, 4). (B) Heparitinase treatment (H'ase) did not cause any mobility shift. In contrast, by chondroitinase ABC treatment (Ch'ase), three additional bands appeared (120 kD, 130 kD and 145 kD, asterisks).

Figure 3. Immunostaining of **wild type embryos** with anti-Mp antibody; lateral view (A), ventral views (B-F) and dorsal view (G). Anterior is left. (A) At stage 8, Mp (blue) appears at the sites of invagination in the anterior and posterior midgut rudiment (arrowheads), and in the procephalic neuroblasts of anterior part in a segmental cellular fashion (arrows). (B) At stage 14, Mp is expressed in a subset of the cells in the PNS (arrows) and in the cells along the midline in the CNS (arrowhead). (C) Left: Confocal analysis of Mp positive cells (red) on A5-A8 segments revealed their relative localization to the neuropile (green). Right: Depth code of the Mp positive cells in the same image. Mp positive cells on the midline (arrows) are more ventrally located than those of the paired ones (arrowhead). Midline is indicated by white bars. (D) Engrailed expressing cells (brown) exist adjacent to Mp expressing cells but they do not colocalize. (E) At stage 16, Mp appeared as a ladder pattern, suggesting it is expressed in interneurons (arrow). (F) At different focal plane, Mp is seen at visceral muscle (arrowhead). (G) On the dorsal side, Mp expression is prominent in the cardioblasts in the heart (bracket) and in the PNS (arrows). Scale bar: 50  $\mu$ m. (H) Schematic representation of the heart (bracket) in

(G). Mp (black shadow) is seen in the cardioblasts of the heart region (orange circle), but is absent in those of the aorta (green circle) and in the ostia (blue oval), the inflow tract of the heart.

Figure 4. Characterization of Mp mutants and their multiple phenotypes. (A) Larval mRNAs from wild type (lane 1, 4, 7, 10),  $mp^{f07253}/mp^{f07253}$  (lane 2, 5, 8, 11) and  $mp^{f03008}/mp^{f03008}$  (lane 3, 6, 9, 12) were reverse transcribed and amplified for *mp*-A (lane 1, 2, 3), *mp*-B (lane 4, 5, 6), the *mp* endostatin region (ES-AS4: lane 7, 8, 9) and *rp49*, a gene encoding a ribosomal protein, as a control (lane 10, 11, 12). The *mp* gene expression level in each homozygote was estimated according to the band intensity of endostatin region (Wild type:  $mp^{f07253}/mp^{f07253}$ :  $mp^{f03008}/mp^{f03008} = 17.6: 1.4: 1$ ). (B) Wild type wing. (B') Typical wing phenotype observed in  $mp^{f07253}/mp^{f07253}$ . Note the diffusive marginal region at the L4 and L5 ends (arrows). (C) Wild type flies develop normal tergites. (C') Flies  $mp^{f03008}/mp^{f03008}$  often miss hemitergite (arrow) or fail to fuse hemitergites at the dorsal midline (arrowhead). (B'', C'') The ratios of individual flies with abnormal wings (B'') or with dorsal abdominal segments (C''). WT (n=56), f03008 homo (n=33), f07253/f03008 (n=68), f07253 homo (n=57).

Figure 5. (A) Touch response analysis. Occurrences of each type of response observed in the analysis

(No response: 0; stop: 1; retract: 2; turn away  $<90^\circ$ : 3; turn away  $\geq 90^\circ$ : 4) (top) and the averages of scores of each strain are indicated with S.E.M. (error bars). The numbers of larvae used for this assay were indicated below. (B, B') Morphologies of developing sensory neurons are visualized by immunostaining with 22c10 antibody. Images of whole embryos (top); magnified view of yellow rectangle (bottom). The chordotonal organs in wild type (B, arrowhead) exhibit fine neural structures while blunt morphology in *mp<sup>f07253</sup>/mp<sup>f07253</sup>* (B', arrowhead). (C, C') Fatbodies from third instar larvae stained for lipid accumulation by oil red. Scale bar: 100  $\mu\text{m}$ . Lipid droplets are small and dense in the fatbody of wild type (C) while those are large and sparse in *mp<sup>f07253</sup>/mp<sup>f07253</sup>* (C'). (D, D') Confocal immunofluorescent images of Viking, *Drosophila*  $\alpha 2(\text{IV})$  collagen. Note that the linear cell boundary pattern in wild type (D) is not observed in mutant (D'). (E, E') Ultrastructure of the cell boundary regions formed by three cells in the third instar larval fatbodies. Scale bar: 5  $\mu\text{m}$ . Adjacent cells contact closely with thin intercellular spaces in wild type (E, arrowheads) while those are broadened in *mp<sup>f07253</sup>/mp<sup>f07253</sup>* mutants (E', arrowheads).

Figure 6. Wingless distributions in embryos (A, A') and in the proventriculus of third instar larvae (B, B'). (A) Strong Wingless immunoreactive signals were observed at segmental stripes, at the central midgut constriction (arrow) and at the both ends of midgut (arrowheads) in wild type

embryos. (A') Immunoreactive signals of Wingless were suppressed in  $mp^{f07253}/mp^{f07253}$  embryos. (B) Strong Wingless signal (bracket) observed in the proventriculus of wild type third instar larvae. (B') Diminished Wingless deposition (bracket) in the proventriculus of  $mp^{f07253}/mp^{f07253}$  third instar larvae. (C) Mp protein localization (purple) in relation to *wingless-lacZ* expression site (light blue) in the proventriculus of third instar larva. *wingless* expressing cells lie at the boundary between the ectodermal cell (EC) and the endodermal cells (EN). (C') Summarized illustration of (C). Scale bars: (A, A'), 50  $\mu\text{m}$ ; (B, B', C), 100  $\mu\text{m}$ .

Figure 1  
[Click here to download Figure\(s\): mp\\_fig1v2.pdf](#)

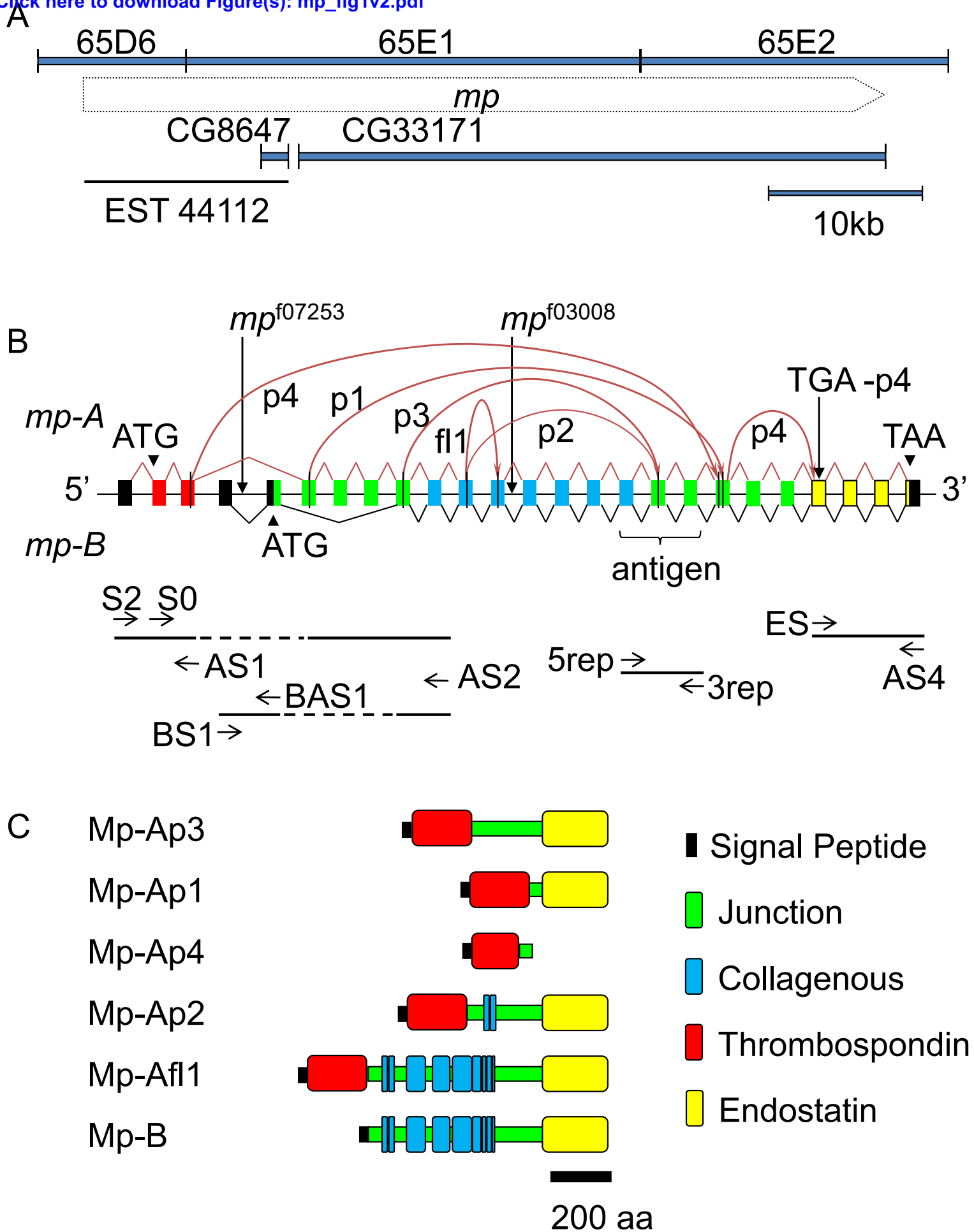


Figure 1

Figure2  
[Click here to download high resolution image](#)

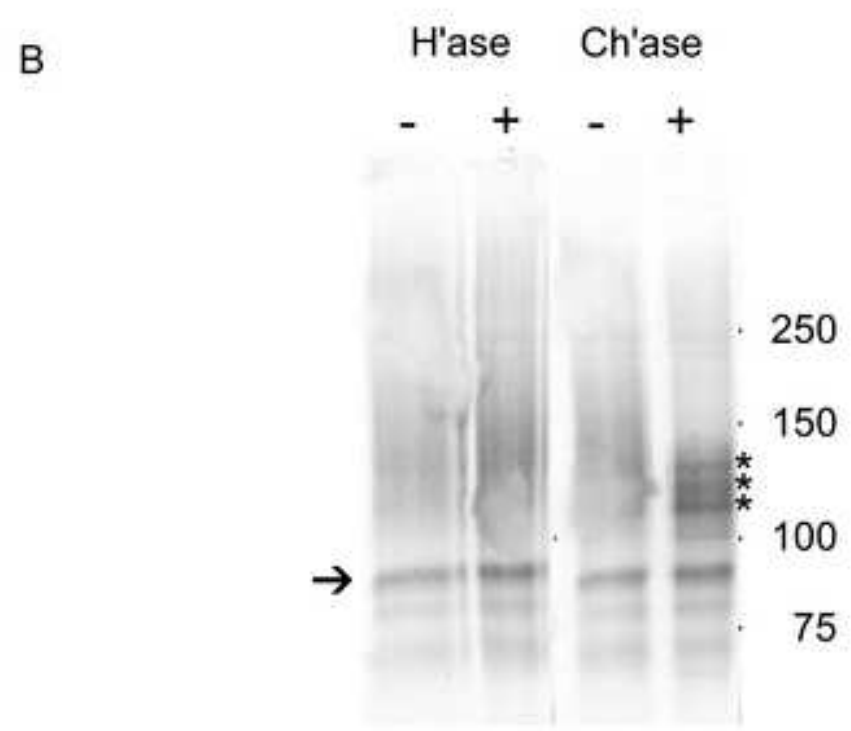
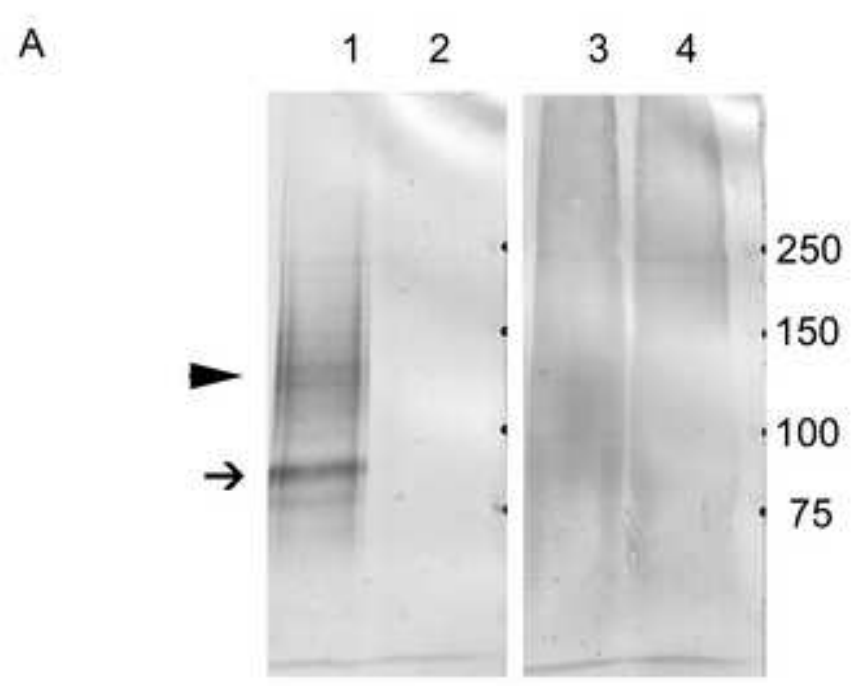


Figure 2

Figure3  
[Click here to download high resolution image](#)

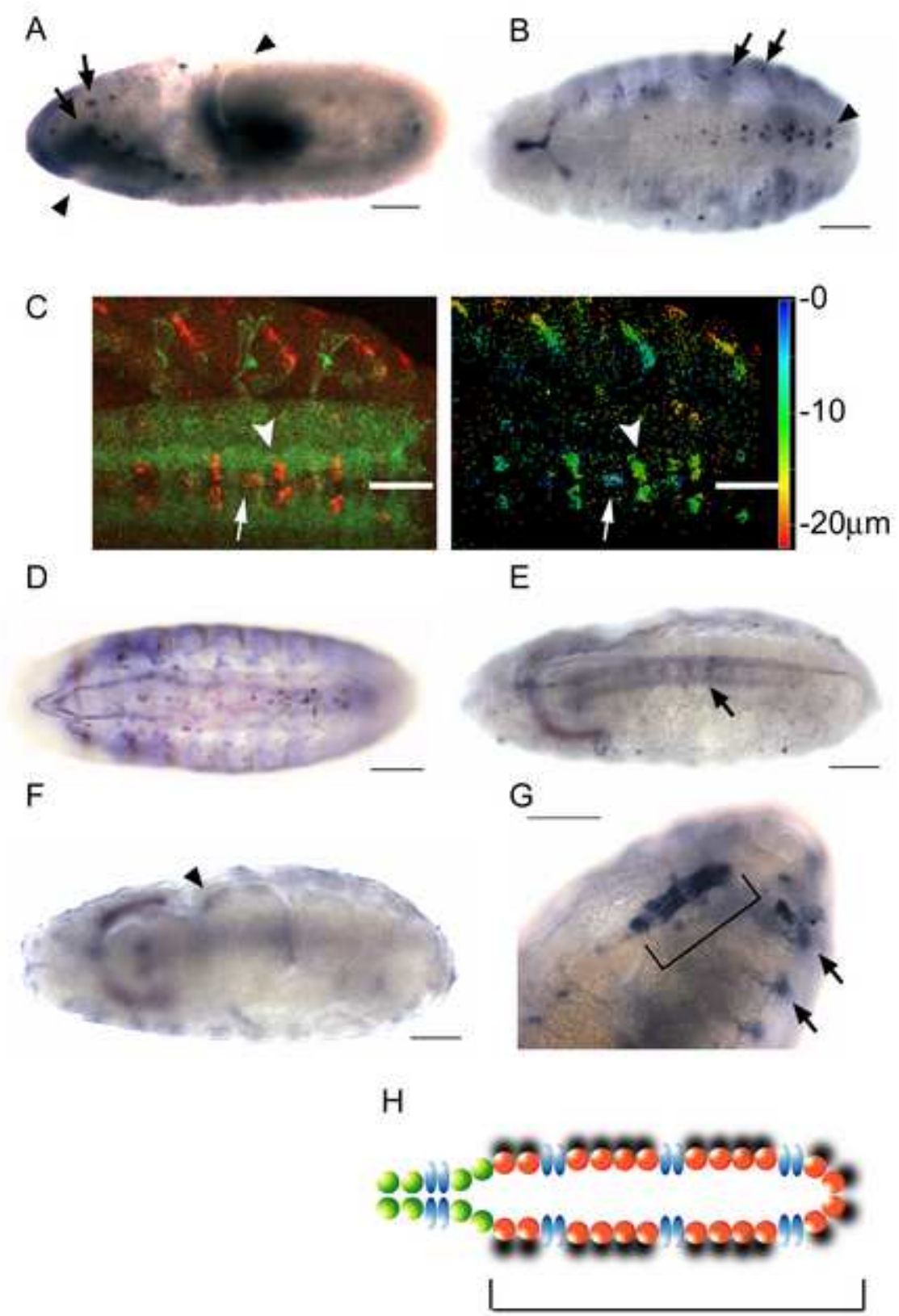


Figure 3

Figure4  
[Click here to download high resolution image](#)

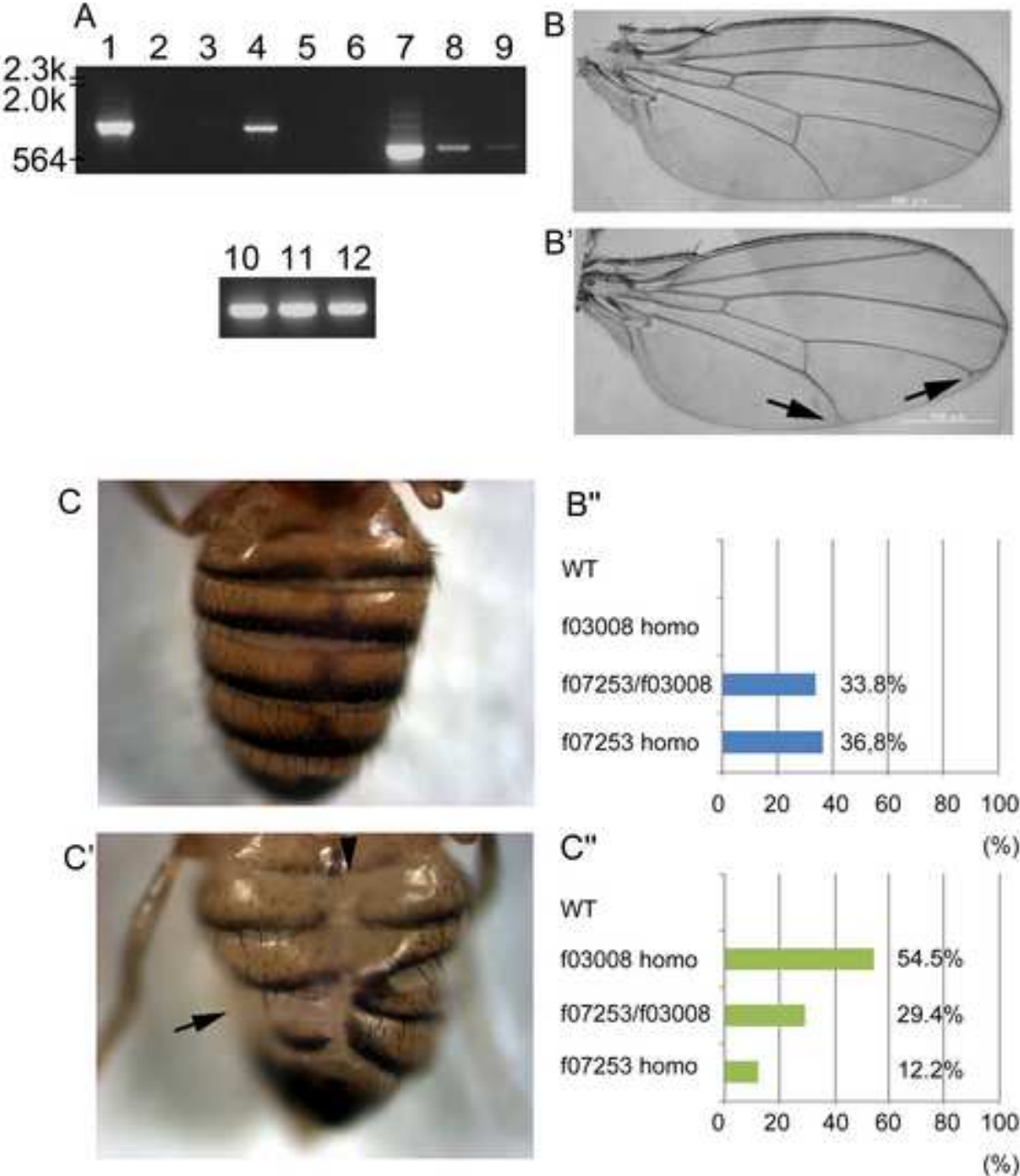


Figure 4



Figure5  
[Click here to download high resolution image](#)

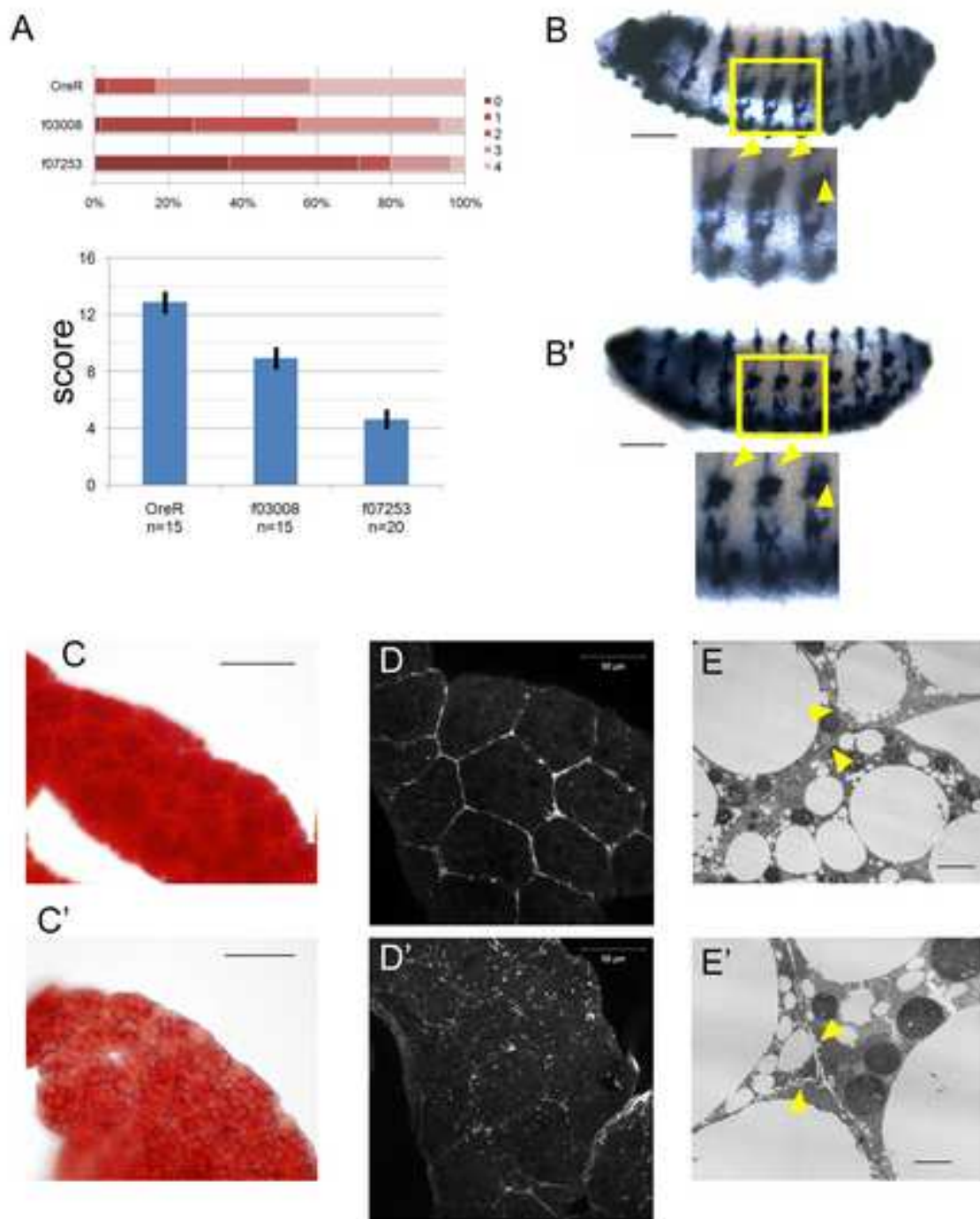


Figure 5

Figure6  
[Click here to download high resolution image](#)

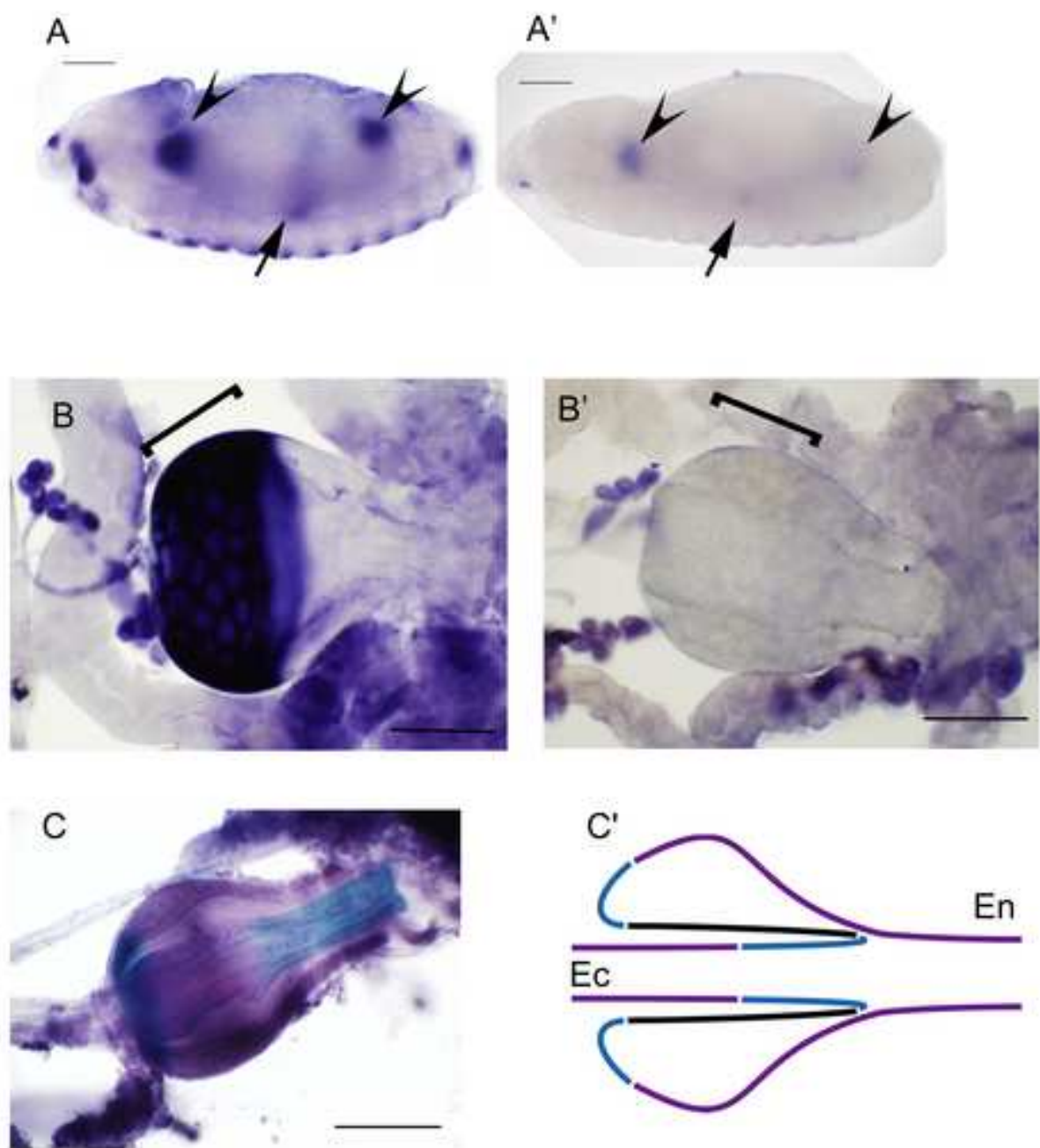


Figure 6